**Buletin Ilmiah Sarjana Teknik Elektro**
Vol. 8, No. 4, August 2026, pp. 1196-1206
ISSN: 2685-9572, DOI: 10.12928/biste.v8i4.17182 

# Fixed-Time Synergetic Control Based Arctic Puffin Optimization for Knee-Exoskeleton Systems

**Huthaifa Al-Khazraji, Laith K. Majeed, Mohammed K. Hamzah, Ahmed Sameer Abdulmohsin**
University of Technology-Iraq, Baghdad, Iraq

## ARTICLE INFORMATION

**Article History:**

Received 23 June 2026
Revised 02 August 2026
Accepted 25 August 2026

**Keywords:**

Exoskeleton System;
Knee Rehabilitation;
Fixed-Time Control;
Synergetic Control;
Arctic Puffin Optimization

**Corresponding Author:**

Huthaifa Al-Khazraji,
University of Technology-Iraq
Baghdad, Iraq.
Email:
huthaifa.k.ibrahim@uotechnology.edu.iq



## ABSTRACT

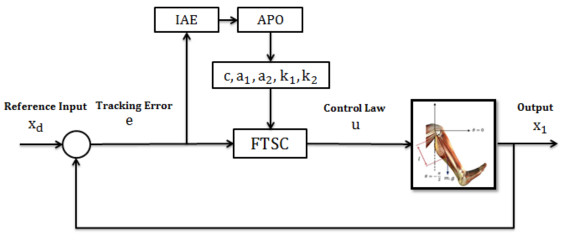


Knee exoskeletons are proving to be highly effective tools for people with leg impairments, using external mechanical support to help their knees move more easily. However, to achieve an accurate trajectory tracking, nonlinearities and torque interaction due human–robot interaction can significantly affect the dynamic performance of the system. In this study, a fixed-time synergetic control (FTSC) strategy is proposed for the motion control of the knee-joint of an exoskeleton robot system. Furthermore, the performance of the proposed FTSC scheme is optimized using the Arctic Puffin Optimization (APO). A comparative study between the FTSC and conventional synergetic control (CSC) is carried out under step and sinusoidal motion-tracking scenarios. The results demonstrate the superior tracking performance of the proposed FTSC compared with the conventional CSC. The Integral Time of Absolute Error (IAE) performance index is selected as a quantitative measurement for improvements. The numerical data of the results reveal that the tracking error of the system controlled by the FTSC is reduced by 37.34% and 79.1% compared to that of the system controlled by the CSC for the unit step and sinusoidal signal inputs respectively. Furthermore, the FTSC demonstrated a substantial enhancement when a parameter variation was augmented in the simulation for the sinusoidal signal inputs.

**Document Citation:**

H. Al-Khazraji, L. K. Majeed, M. K. Hamzah, and A. S. Abdulmohsin, "Fixed-Time Synergetic Control Based Arctic Puffin Optimization for Knee-Exoskeleton Systems," *Buletin Ilmiah Sarjana Teknik Elektro*, vol. 8, no. 4, pp. 1196-1206, 2026, DOI: 10.12928/biste.v8i4.17182.

## 1. INTRODUCTION

The human knee is an important component of the lower limb, responsible of essential activities including walking, running and cycling. However, its function can be significantly impaired by musculoskeletal disorders, traumatic injuries, stroke, and other neurological conditions, leading to reduced mobility, loss of independence, and a diminished quality of life [1][2]. As the global population ages rapidly, individuals experience progressive physiological declines. Reductions in muscle mass, strength, motor function, flexibility, and aerobic capacity collectively impair mobility and overall functional performance [3]. These age-related changes also increase the susceptibility of older adults to musculoskeletal and neurological disorders, further compromising knee function and highlighting the Increasing demand for high-impact restorative and adaptive technologies [4]. To address these issues including the rapid growth of the aging population, the decline in physical capabilities, and the increasing prevalence of musculoskeletal and neurological disorders, exoskeletons have gained significant attention as an emerging technology for mobility assistance and rehabilitation. These devices represent a promising intervention for mitigating these impaired of the human knee. By delivering personalized mechanical support, strength amplification, and motion assistance, these systems augment human movement to restore physical capabilities, thereby enhancing both functional performance and overall quality of life. As human–robot interaction technologies continue to advance, exoskeletons have emerged as an important research area in rehabilitation robotics and assistive engineering [5][6]. They can supply controlled assistive torques to the joints, compensate for muscle weakness, support repetitive rehabilitation training, and improve gait stability and mobility. Consequently, exoskeletons have become increasingly important for elderly users as well as patients recovering from stroke, traumatic injuries, and other mobility-related disorders [7][8].

In the domain of lower-limb assistive technology, knee exoskeletons utilize actuator-driven torque to guide the knee through specific flexion and extension trajectories. The fidelity of both torque generation and trajectory tracking is critical; it dictates not only the efficacy of the physical support but also the wearer's safety, comfort, and natural kinematics. The effectiveness of knee exoskeletons is not only related to the mechanical design, but also to the development of advanced control algorithms. The control system focuses on actuator torque regulation, joint motion coordination, and accurate trajectory tracking with stable and safe human–robot interaction. This coordination of exoskeleton motion with the natural gait of the wearer result in better assistance to the movement, more effective rehabilitation and improved overall comfort for the user [9].

In the literature, several modeling of knee exoskeleton systems have been developed, and a variety of control strategies have been proposed to address different application scenarios. For example, Touati *et al*. [10] proposed proportional, integral, and derivative (PID) controller for lower limbs exoskeleton system. The controller parameters were designed based on the linearized system model to ensure satisfactory dynamic performance and accurate system response. The performance of the system with the PID controller was evaluated based on the sinusoidal trajectory input. The error between the knee's angular position and the desired angular position was fluctuated between -0.01 and 0.07 rad. Chevalier *et al*. [11] developed a fractional-order proportional-integral (FOPI) controller for knee exoskeleton motion control. The controller was designed using a linearized model of the knee exoskeleton, while its parameters were determined through a model-based tuning method. Simulation results demonstrated that the proposed FOPI controller achieved superior performance compared with the conventional integer-order PI controller. Li *et al*. [12] proposed a control strategy for knee exoskeletons operating under time-varying inertial and damping parameters. The controller was developed based on the zhang dynamics (ZD) framework and incorporated a double ZF to guarantee the exponential convergence of the knee joint angle tracking error to zero. Konyak *et al*. [13] proposed an optimal fuzzy-PID controller for the knee exoskeleton system. The fuzzy logic controller was used to tune the gains of PID based on the joint angle tracking error and its rate of change. The class topper optimization (CTO) was used for optimizing the membership functions of the fuzzy controller. Several simulation scenarios were used to verify the effectiveness of the proposed control strategy. In the work of Waheed and Humaidi [14], sliding mode control (SMC) was implemented to achieve trajectory tracking for a knee exoskeleton system. The whale optimization algorithm (WOA) was adopted to optimize the controller design parameters, thereby enhancing the overall performance of the SMC scheme. A comparative study based on the root mean square error (RMSE) as an evaluation metric is carried out under sin-wave input as desired trajectory. Based on the simulation results, the RMSE (0.0297) of the optimized SMC was less than the RMSE (0.0436) in the non-optimized SMC. The robust stabilization presented in [15] is achieved through the application of Lyapunov theory, yielding a set of linear matrix inequality (LMI) conditions that ensure the stability of the position tracking error. The mathematical derivation incorporates Young's inequality, the Schur complement, the S-procedure, congruence transformations, and the matrix inversion lemma. A terminal synergetic control (TSC) strategy for angular position tracking of a lower-limb exoskeleton was presented by Al-Khazraji *et al* [16]. The controller parameters were optimally tuned using the cheetah optimizer (CO) algorithm with the RMSE adopted as the objective function. The proposed method exhibited superior tracking performance compared with the conventional synergetic control (CSC) technique. The numerical value of the RMSE based on the simulation results reveals that the TSC is reduced RMSE by 14.9% as compared to CSC. In addition, in the presence of external disturbances, the RMSE is reduced by 39.1%.

Previous studies have demonstrated that various control strategies can effectively improve the performance of this system. However, to the best of the authors' knowledge, fixed-time synergetic control (FTSC) has not been applied to this system. Therefore, this work fills this research gap by developing and evaluating a FTSC scheme. The superior performance of FTSC comes from its fixed-time convergence property, which accelerates error reduction both when the tracking error is large and when it is close to zero. Consequently, FTSC achieves faster response, smaller tracking errors, and enhanced robustness compared with classical synergetic control. Furthermore, the arctic puffin optimization (APO) algorithm is employed to optimally tune the parameters of the FTSC, thereby enhancing the overall control performance of the proposed scheme.

## 2. MATHEMATICAL MODEL

This section introduces the mathematical model of the single-joint knee-exoskeleton system. The goal of the control system is to generate the appropriate knee joint torque that compensates for gravitational and loading forces, thereby assisting the user in performing natural knee movements. The mechanical configuration of the proposed knee exoskeleton is shown in Figure 1. It consists of two rigid links representing the thigh and shank-foot segments. The thigh link is actuated by a motor and fixed along the x-axis, while the shank-foot link rotates about the knee joint to perform flexion and extension. The angular displacement θ is limited to the range of 0–90, which corresponds to the intended operating range of the exoskeleton [14][15].

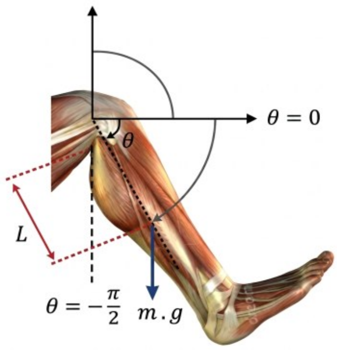


**Figure 1.** Exoskeleton system [14][15]

The dynamic model of the knee exoskeleton is derived using the Lagrangian formulation. The corresponding governing equation is given by [17]:

$$\frac{d}{dt}\left(\frac{\partial L}{\partial t}\right) - \left(\frac{\partial L}{\partial t}\right) = \tau_t \tag{1}$$

where L is the Lagrangian component and $\tau_t$ represents the external total torque applied to the system. The total external torque is composed of two components, as defined in (2): the resistive torque, which accounts for the solid and viscous friction present in the system, and the active torque generated by the actuator and applied to the exoskeleton joint.

$$\tau_t = \tau_r + \tau \tag{2}$$

where $\tau_r$ are the resistive torques and τ is the control torque produced by the DC motor. The system's resistive torque is expressed as follows:

$$\tau_r = -f_b\dot{\theta} - f_s\, sign\,(\dot{\theta}) \tag{3}$$

where $f_b\dot{\theta}$ is the viscous damping torque of the exoskeleton system, $f_s\, sign\,(\dot{\theta})$ is the solid friction torque of the system. The Lagrangian has the following definition:

$$L = E_{ke} - K_{ge} \tag{4}$$

The system's elements' kinetic and gravitational energy are represented by the symbols $E_{ke}$ and $K_{ge}$, respectively [14].

$$E_{ke} = \frac{1}{2} J\dot{\theta} \tag{5}$$

where $J$ denotes the inertia of the system.

$$E_{ge} = mgl(1 - sin(\theta)) \tag{6}$$

where the symbols $m, g, l$ stand for the leg and exoskeleton system mass, gravity-induced acceleration, and the separation between the knee joint and the center of gravity, respectively. The combined system components' dynamic model can be expressed as follows [16]:

$$J\ddot{\theta} = mgl\,cos\,(\theta) - f_b\dot{\theta} - f_s\,sign(\dot{\theta}) + \tau \tag{7}$$

Let $\tau_m = mgl$, Eq. (8) can be write as follows:

$$J\ddot{\theta} = \tau_m\,cos\,(\theta) - f_b\dot{\theta} - f_s\,sign(\dot{\theta}) + \tau \tag{8}$$

For control design purposes, let $x_1$ and $x_2$ denote the angular position θ and angular velocity $\dot{\theta}$, respectively. Consequently, the state variable equations of the system are given by:

$$\dot{x}_1 = x_2 \tag{9}$$

$$\dot{x}_2 = \frac{1}{J}[\tau - f_b x_2 - f_s\,sign(x_2) + \tau_m\,cos\,(x_1)] \tag{10}$$

Eq. (10) can be revised as follows:

$$\dot{x}_2 = F_x + bu \tag{11}$$

where

$$F_x = \frac{-f_b x_2 - f_s\,sign(x_2) + \tau_m\,cos\,(x_1)}{J}$$

$$b = \frac{1}{J}$$

## 3. FIXED-TIME SYNERGETIC CONTROL

Model-based control techniques have been widely employed in the control of a broad range of nonlinear and dynamic systems due to their ability to explicitly incorporate system dynamics into the controller design [18]-[21]. Synergetic control (SC) is a simple yet robust nonlinear model-based control method that has been extensively employed in the literature [22]-[26]. Its major advantage lies in its ability to handle nonlinear systems directly, thereby avoiding the need for linearization during controller design. The objective of the controller design is to make the knee-exoskeleton system follows the trajectory tracking accurately. Let's define e as the error between the tracking errors as: $e_1 = x_1 - x_d$ and $e_2 = x_2 - \dot{x}_d$. The initial stage of the synergetic control design involves choosing an appropriate macro variable, as this selection directly determines the structure of the control law and ensures that the system follows the prescribed reference trajectory. Choose the synergetic macro-variable:

$$\varphi = e_2 + ce_1 \tag{12}$$

Derivative of the macro-variable: $\dot{\varphi} = \dot{e}_2 + c\dot{e}_1$. Since $e_2 = \dot{e}_1$ and $\dot{e}_2 = F_x + bu - \ddot{x}_d$, then:

$$\dot{\varphi} = F_x + bu - \ddot{x}_d + ce_1 \tag{13}$$

Unlike the conventional synergetic control approach, the macro-variable dynamics are designed using the fixed-time concept to achieve convergence within a predefined upper time bound independent of the initial states. Therefore, to assure that the state trajectories travel toward the desired manifolds with a fixed-time dynamics, let's define the following [27][28]:

$$\dot{\varphi} = -k_1|\varphi|^{a_1}\, sgn(\varphi) - k_2|\varphi|^{a_2}\, sgn(\varphi) \tag{14}$$

where $0 < a_1 < 1$ , $a_2 > 1$ , $k_1, k_2 > 0$

By substituting $\dot{\varphi}$ in Eq. (13) into Eq. (14) gives:

$$F_x + bu - \ddot{x}_d + ce_1 = -k_1|\varphi|^{a_1}\, sgn(\varphi) - k_2|\varphi|^{a_2}\, sgn(\varphi) \tag{15}$$

Select $u$ as

$$u = \frac{1}{b}\left(-F_x + \ddot{x}_d - ce_1 + k_1|\varphi|^{a_1}\, sgn(\varphi) + k_2|\varphi|^{a_2}\, sgn(\varphi)\right) \tag{16}$$

Proof stability: define the Lyapunov function as:

$$V = \frac{1}{2}\varphi^2 \tag{17}$$

Differentiate V with time: $\dot{V} = \varphi\dot{\varphi}$ and substitute $\dot{\varphi}$ as given in Eq. (14) gives:

$$\dot{V} = \varphi\left(-k_1|\varphi|^{a_1}\, sgn(\varphi) - k_2|\varphi|^{a_2}\, sgn(\varphi)\right) \tag{18}$$

Since $\varphi\, sgn(\varphi) = |\varphi|$, $\dot{V}$ can be rewrite as:

$$\dot{V} = -k_1|\varphi|^{a_1+1} - k_2|\varphi|^{a_2+1} \tag{19}$$

From Eq. (17), it can be observe $|\varphi| = \sqrt{2V}$ , then Eq. (19) becomes:

$$\dot{V} = -k_1(2V)^{\frac{a_1+1}{2}} - k_2(2V)^{\frac{a_2+1}{2}} \tag{20}$$

Let $\rho_1 = k_1 2^{\frac{a_1+1}{2}}$ and $\rho_2 = k_1 2^{\frac{a_2+1}{2}}$, this yields:

$$\dot{V} = -\rho_1 V^{\frac{a_1+1}{2}} - \rho_2 V^{\frac{a_2+1}{2}} \tag{21}$$

Notice $\frac{a_1+1}{2} < 1$ and $\frac{a_2+1}{2} > 1$, this matches the standard fixed-time Lyapunov inequality $\dot{V} = -\rho_1 V^p - \rho_2 V^q$ where $0 < p < 1$ and $q > 1$. According to Polyakov's fixed-time stability theorem [29], the equilibrium $\varphi = 0$ is globally fixed-time stable, and the settling time is bounded by: $T \le \frac{1}{\rho_1(1-p)} + \frac{1}{\rho_2(q-1)}$ which is independent of the initial conditions.

## 4. ARCTIC PUFFIN OPTIMIZATION

Swarm optimization techniques are superior to other optimization methods in that they are fast and simple in implementing convergence as well as not being limited in distinguishing the objective function, self-organized, and in addition to their strength in global search [30]-[33]. Hence, researchers are interested in adopting these algorithms to solve a large number of optimization problems in practical applications including optimization the controller design parameters [34]-[42]. In this work, arctic puffin optimization (APO) is employed to tune the parameters of the fixed-time synergetic control (FTSC). APO, introduced by Wang *et al.* in 2024 [43], is a swarm intelligence-based metaheuristic algorithm inspired by the hunting and navigation behavior of Arctic puffins. By maintaining a balance between exploration and exploitation throughout the optimization process, APO efficiently searches nonlinear parameter spaces to obtain high-quality solutions for complex optimization problems.

APO has demonstrated strong performance in multi-objective controller tuning and various engineering optimization problems, outperforming or remaining competitive with several existing metaheuristic algorithms [44]-[45]. The algorithm's power lies in deriving collective intelligence from simple rules of movement. APO alternates between two search mechanisms: the flight phase, which enhances exploration by dispersing individuals across the search space, and the dive phase, which improves exploitation by conducting a more intensive search near high-quality solutions [46]. Within APO framework, each the position in the population $p_i$ is updated to minimize the fitness function $f(p_i)$. The mechanism of updating is express by [47]:

$$p_i^{k+1} = p_i^k + \sigma_1 r_1 p_r^k + \sigma_2 r_2\left(p_b - p_i^k\right) \tag{22}$$

where $p_i^{k+1}$ is the new position of $p_i^k$. $p_b$ is the position of the best value, $x_r^k$ is the random position in the population. $r_1$ and $r_1$ are two random values between 0 and 1 for the k-th iteration. $\sigma_1$ and $\sigma_2$ weight/scale parameters. The term $(\sigma_1 r_1 p_r^k)$ represents the exploration searching process whereas the term $(\sigma_2 r_2(p_b - p_i^k))$ represents exploitation searching process. Algorithm 1 presents the pseudocode of APO.

| **Algorithm1. APO Pseudcoode** |
|---|
| 1. Input |
| $T_m$: Iteration number, $N_p$: Population size, Objective function, $\sigma_1$ and $\sigma_2$ |
| 2. Initialization |
| Position of population is assigned randomly |
| Evaluate the objective function and choose the best solution |
| 3. Loop: |
| while $k < T_m$ |
| The position $p_i^k$ is updated using Eq. (22) |
| Selection best solution and update $p_b$ |
| $k = k + 1$ |
| End while |
| 4. Print the Best Solution |

## 5. COMPUTER SIMULATION RESULTS

The numerical simulation using MATLAB has been conducted to evaluate the effectiveness of the proposed fixed-time synergetic control (FTSC). As shown in Figure 1, the exoskeleton leg is designed to operate within an allowable range of motion from 0 rad (horizontal position) to $-\pi/2$ $(-1.57)$ $rad$ (vertically downward position). The dynamics of the knee-exoskeleton system, as described by Eq. (9) to Eq. (10), are coded to perform the computer simulation. The parameters of knee-exoskeleton system as follows: $J = 0.348\ K_g.m^2$, $f_s = 0.998\ N.m$, $f_v = 0.872\ N.m.s/rad$, and $\tau_g = 3.44\ N.m$ [14]. The controlled system is simulated with a -0.3 rad initial position and zero initial velocity. The arctic puffin optimization (APO) is utilized to tune parameters $(c, a_1, a_2, k_1 and\ k_2)$ of the FTSC's control law in the Eq. (16). The Integral of Absolute Error (IAE) between the output $x_1$ and the desired reference signal $x_d$ is utilized as cost function as given in Eq. (23) [48]-[50].

$$IAE = \int_{t=0}^{t=t_s} t|e|dt \tag{23}$$

where $t_s$ means the period of the simulation time. The population size $(N_p)$ of the APO is 20 and the number of Iterations $(T_m)$ 30. The configuration of the FTSC optimized by APO for the knee-exoskeleton system is shown in Figure 2.

The optimal values of the design parameters of the FTSC found as follows: $c = 14, a_1 = 10, a_2 = 8, k_1 = 0.5\ and\ k_2 = 1.5$. To comprehensively evaluate the proposed FTSC under practical operating conditions, two motion scenarios are considered and compared with the conventional synergetic control (CSC). The first scenario investigates the static position tracking capability, in which the exoskeleton leg is commanded to move from its initial position to a desired fixed position and maintain that posture. This scenario represents tasks such as leg positioning and posture assistance. To emulate this operation, a step reference input of 0 rad is applied with 2 s simulation time, corresponding to a moderate upward movement of the exoskeleton leg within its allowable range of motion. The second scenario evaluates the dynamic trajectory tracking performance by employing a time-varying reference that represents continuous leg movement during activities such as gait and rehabilitation exercises. Accordingly, the desired trajectory is selected as $x_{d(t)} = -0.3 - 0.3sin(t)$ with 20 s simulation time, ensuring that the reference remains within the allowable range of motion while providing a realistic periodic leg movement. Moreover, for each motion scenario, the controller is assessed under three operating conditions. The first condition considers the nominal system without parameter variations or external disturbances to evaluate the basic tracking performance. The second condition investigates the robustness of the controller against parametric uncertainty. The third condition evaluates the disturbance rejection capability by applying an external disturbance torque to the system. Consequently, both the static position tracking and dynamic trajectory tracking scenarios are examined under all three operating conditions to provide a comprehensive assessment of the proposed controller in terms of tracking accuracy, robustness, and disturbance rejection.

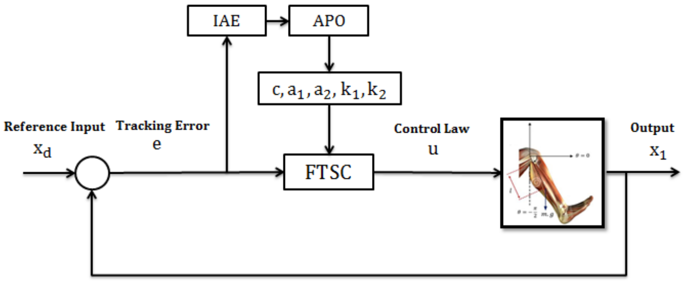


**Figure 2.** Proposed FTSC tuned by APO for knee-exoskeleton system

## 5.1. Normal Operation

For normal operation evaluation, Figure 3 and Figure 4 present the position responses and tracking errors for both the step-input and time-varying trajectory reference tracking cases, and Table 1 lists the corresponding IAE values. Both cases show better tracking performance of the proposed FTSC in comparison with CSC. For the step-input case, the FTSC achieves an IAE of 0.52, compared with 0.83 for the CSC, representing a 37.34% reduction in the IAE. Similarly, for the time-varying trajectory, the FTSC yields an IAE of 0.0075, which is significantly lower than the 0.0359 obtained with the CSC, corresponding to a 79.1% reduction. These results confirm the effectiveness of the proposed FTSC in enhancing tracking accuracy under both operating conditions.

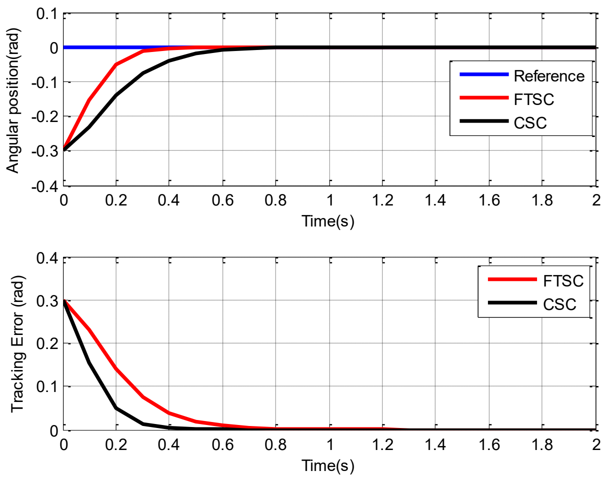


**Figure 3.** Angular position response and tracking error for step reference (Normal Operation)

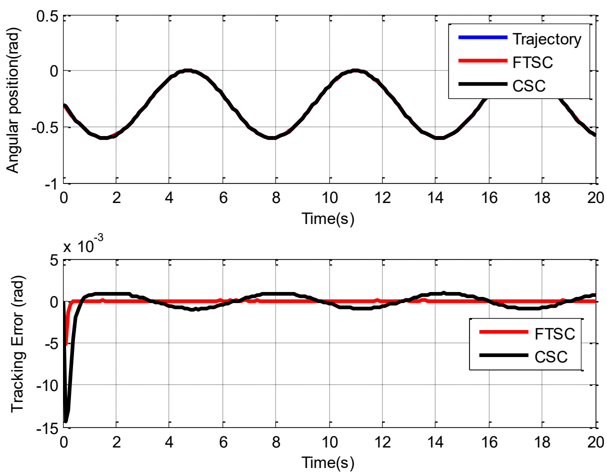


**Figure 4.** Angular position response and tracking error for time-varying reference (Normal Operation)

**Table 1.** IAE for normal operation

| Controller | IAE | |
|---|---|---|
| | Step | Time-varying |
| FTSC | 0.52 | 0.0075 |
| CSC | 0.83 | 0.0359 |

## 5.2. Uncertainty

In this case, 20% reduction in the inertia of the system was assumed to evaluate the robustness of the FTSC to uncertainty. The position responses and tracking errors for both the step-input and time-varying trajectory tracking scenarios are depicted in Figure 5 and Figure 6, respectively, whereas the corresponding IAE values are reported in Table 2. It can be seen that the performance of the step response is almost the same as that obtained under a nominal condition with a 20% reduction in the system inertia. Since the step reference approaches to a constant equilibrium, both controllers can compensate well for the moderate parameter variation, keeping the tracking accuracy almost same. Thus the IAE values for the respective case are not changed. In contrast, the time-varying reference continuously excites the system dynamics, making the tracking performance more sensitive to variations in the inertia. Since inertia directly influences the angular acceleration, the parameter mismatch affects the controller throughout the tracking process, resulting in different IAE values. As shown in Table 2, the proposed FTSC achieves an IAE of 0.0097, compared with 0.1582 for the CSC, demonstrating its superior robustness against inertia uncertainty during dynamic trajectory tracking.

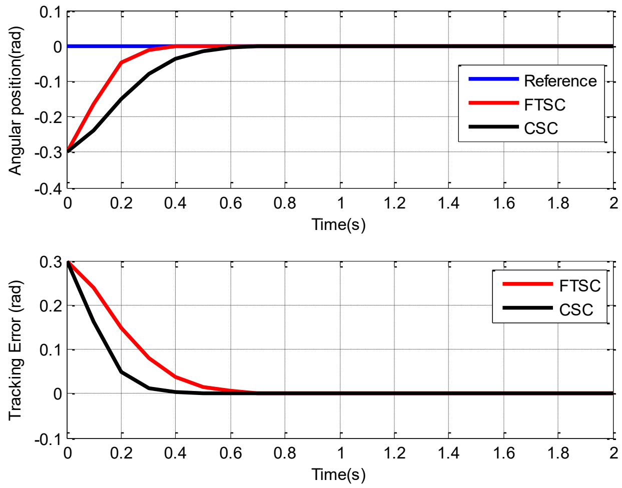


**Figure 5.** Angular position response and tracking error for step reference (Uncertainty)

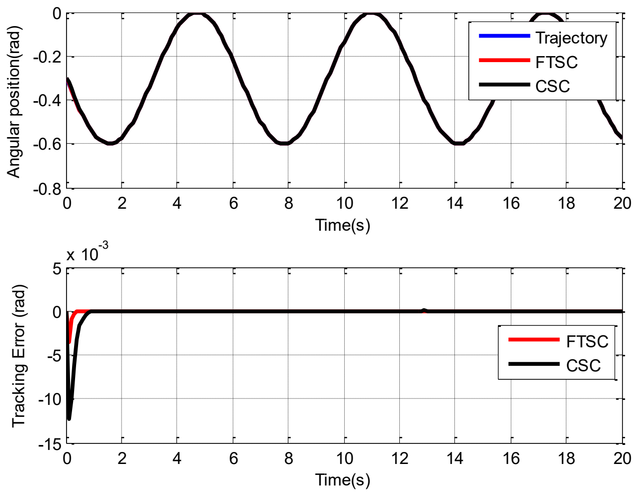


**Figure 6.** Angular position response and tracking error for time-varying reference (Uncertainty)

**Table 2.** IAE for uncertainty

| Controller | IAE | |
|---|---|---|
| | **Step** | **Time-varying** |
| FTSC | 0.52 | 0.0097 |
| CSC | 0.83 | 0.1582 |

## 6. CONCLUSIONS

This study presents the design of a fixed-time synergetic control (FTSC) for step and sinusoidal motion-tracking control of knee-joint exoskeleton system. The proposed FTSC is compared with conventional synergetic control (CSC). The comparison in performance has been conducted between two control schemes in terms of reducing the tracking error via numerical simulation. Overall, the proposed FTSC achieves better tracking performance than the conventional CSC under nominal operating conditions. Its main advantage, however, is evident under parameter uncertainty, where it exhibits considerably greater robustness, particularly during dynamic trajectory tracking. These results indicate that the FTSC is more effective in maintaining accurate trajectory tracking despite variations in the system inertia, making it a more reliable control strategy for practical exoskeleton applications. Future work could have different directions. For example, the proposed system can be validated experimentally to assess its practical performance under real operating conditions. In addition, adaptive control strategies can be incorporated to automatically adjust the controller parameters in response to variations in user requirement. Another promising direction is to extend the proposed control framework from a single-joint knee exoskeleton to a multi-joint lower-limb exoskeleton, such as an integrated knee–ankle system, to achieve coordinated motion control.

## REFERENCES

[1] M. S. Fragala, E. L. Cadore, S. Dorgo, M. Izquierdo, W. J. Kraemer, M. D. Peterson, and E. D. Ryan, "Resistance training for older adults: position statement from the national strength and conditioning association," *The Journal of Strength & Conditioning Research*, vol. 33, no. 8, pp. 2019-2052, 2019, https://doi.org/10.1519/JSC.0000000000003230.

[2] L. Fan, L. Yan, and J. Xiao, "Study on the Fuzzy Control Algorithm for Knee Exoskeleton Based on Co-simulation," *In International Conference on Mechatronics and Intelligent Robotics*, pp. 1123-1129, 2018, https://doi.org/10.1007/978-3-030-00214-5_137.

[3] M. Cristea, G. G. Noja, P. Stefea, and A. L. Sala, "The impact of population aging and public health support on EU labor markets," *International journal of environmental research and public health*, vol. 17, no. 4, p.1439, 2020, https://doi.org/10.3390/ijerph17041439.

[4] M. Tieland, I. Trouwborst, and B. C. Clark, "Skeletal muscle performance and ageing," *Journal of cachexia, sarcopenia and muscle*, vol. 9, no. 1, pp.3-19, 2018, https://doi.org/10.1002/jcsm.12238.

[5] G. Li, X. Liang, H. Lu, T. Su, and Z.G. Hou, "Development and Validation of a Self-Aligning Knee Exoskeleton with Hip Rotation Capability," *IEEE Transactions on Neural Systems and Rehabilitation Engineering*, vol. 32, pp. 472-481, 2024, https://doi.org/10.1109/TNSRE.2024.3354806.

[6] H. S. Majeed, S. K. Kadhim, and A. A. Jaber, "Design of a sliding mode controller for a prosthetic human hand's finger," *Engineering and Technology Journal*, vol. 40, no.1, pp.257-266, 2022, https://doi.org/10.30684/etj.v40i1.1943.

[7] J. H. Kim, M. Shim, D. H. Ahn, B. J. Son, S. Y. Kim, D. Y. Kim, Y. S. Baek, and B. K. Cho, "Design of a knee exoskeleton using foot pressure and knee torque sensors," *International Journal of Advanced Robotic Systems*, vol. 12, no. 8, p.112, 2015, https://doi.org/10.5772/60782.

[8] A. M. Khomami, and F. Najafi, "A survey on soft lower limb cable-driven wearable robots without rigid links and joints," *Robotics and Autonomous Systems*, vol. 144, p.103846, 2021, https://doi.org/10.1016/j.robot.2021.103846.

[9] Y. Sun, Y. Tang, J. Zheng, D. Dong, X. Chen, and L. Bai, L., "From sensing to control of lower limb exoskeleton: A systematic review," *Annual Reviews in Control*, vol. 53, pp.83-96, 2022, https://doi.org/10.1016/j.arcontrol.2022.04.003.

[10] N. Touati, I. Saidi, and H. B. H. Mbarek, "PID control of a lower limb rehabilitation exoskeleton," *Przegląd Elektrotechniczny*, vol. 2024, no. 6, pp. 290-293, 2024, https://doi.org/10.15199/48.2024.06.60.

[11] A. Chevalier, C.M. Ionescu, and R. De Keyser, "Analysis of robustness to gain variation in a fractional-order PI controller for knee joint motion" In *ICFDA'14 International Conference on Fractional Differentiation and Its Applications*, pp. 1-6, 2014, https://doi.org/10.1109/ICFDA.2014.6967359.

[12] Z. Li, W. Ma, Z. Yin, and H. Guo, "Tracking control of time-varying knee exoskeleton disturbed by interaction torque," *ISA transactions*, vol. 71, pp.458-466, 2017, https://doi.org/10.1016/j.isatra.2017.08.004.

[13] N. M. Konyak, D. Acharya, and D. K. Das, "Development of Optimal Fuzzy-PID Controller for an Assistant Human Knee Exoskeleton System," In *TENCON IEEE Region 10 Conference (TENCON)*, pp. 777-782, 2023, https://doi.org/10.1109/TENCON58879.2023.10322520.

[14] Z. A. Waheed, and A. J. Humaidi, "Whale Optimization Algorithm Enhances the Performance of Knee-Exoskeleton System Controlled by SMC," *Iraqi journal of computers, communications, control and systems engineering*, vol. 23, no. 2, pp.125-135, 2023, https://doi.org/10.33103/uot.ijccce.23.2.10.

[15] S. Jenhani, H. Gritli, and J. Narayan, "Robust Position Control of a Knee-Joint Rehabilitation Exoskeleton Using a Linear Matrix Inequalities-Based Design Approach," *Applied Sciences*, vol. 15, no. 1, p.404, 2025, https://doi.org/10.3390/app15010404.

[16] H. Al-Khazraji, A. K. Ahmend, A.I. Abdulkareem, and A.J. Humaidi, "Terminal synergetic control based cheetah optimizer for knee-exoskeleton systems," *Serbian Journal of Electrical Engineering*, vol. 22, no. 3, pp.437-452, 2025, https://doi.org/10.2298/SJEE240924006A.

[17] K. Al-Badri, H. Dulaimi, H. Al-Khazraji, and A.J. Humaidi, "Adaptive Neural Network Control for Load-Varying Two-Link Robots Using Honey Badger Optimization," *Journal of Robotics and Control (JRC)*, vol. 6, no. 2, pp.1061-1068, 2025, https://doi.org/10.18196/jrc.v6i2.26370.

[18] S. El Aamery, R. El Bachtiri, and R. El Idrissi, "A Novel Hybrid Artificial Neural Network and Finite-Time Sliding Mode Control Strategy for MPPT in PV Water Pumping Systems with Real-Time Implementation," *Arabian Journal for Science and Engineering*, vol. 51, pp.1-23, 2025, https://doi.org/10.1007/s13369-025-10901-8.

[19] B. Godspower, D. E. A. Mansour, A. Nada, and T. F. Megahed, "Robust Super-Twisting Control of Active Magnetic Bearing," In *2024 25th International Middle East Power System Conference (MEPCON)*, pp. 1-6, 2024, https://doi.org/10.1109/MEPCON63025.2024.10850321.

[20] Z. Jin, X. Sun, G. Lei, Y. Guo, and J. Zhu, "Sliding mode direct torque control of SPMSMs based on a hybrid wolf optimization algorithm," *IEEE Transactions on Industrial Electronics*, vol. 69, no. 5, pp.4534-4544, 2021, https://doi.org/10.1109/TIE.2021.3080220.

[21] A. Naderolasli, "Constrained super-twisting sliding-mode controller for beam and ball nonlinear system stabilization with limited field-of-view constraints," *Iranian Journal of Science and Technology, Transactions of Electrical Engineering*, vol. 49, no. 4, pp.1645-1659, 2025, https://doi.org/10.1007/s40998-025-00841-2.

[22] J. Qian, K. Li, H. Wu, J. Yang, and X. Li, Synergetic Control of GridConnected Photovoltaic Systems," *International Journal of Photoenergy*, vol. 2017, no. 1, p.5051489, 2017, https://doi.org/10.1155/2017/5051489.

[23] N. Chiem, "Cascade Control for Trajectory-Tracking Mobile Robots Based on Synergetic Control Theory and Lyapunov Functions," *Control Systems and Optimization Letters*, vol. 3, no. 1, 14-19, 2025, https://doi.org/10.59247/csol.v3i1.169.

[24] B. Deffaf, H. Farid, H. Benbouhenni, S. Medjmadj, and N. Debdouche, "Synergetic control for three-level voltage source inverter-based shunt active power filter to improve power quality," *Energy Reports*, vol. 10, pp.1013-1027, 2023, https://doi.org/10.1016/j.egyr.2023.07.051.

[25] F.R. Al-Ani, O.F. Lutfy, and H. Al-Khazraji, "Optimal synergetic and feedback linearization controllers design for magnetic levitation systems: a comparative study," *Journal of Robotics and Control (JRC)*, vol. 6, no. 1, pp.22-30, 2025, https://doi.org/10.18196/jrc.v6i1.24452.

[26] A. K. Abbas, and S. K. Kadhim, "Eliminating Chattering in Prosthetic Fingers Using Classic Synergetic Control," *Journal Europeen des Systemes Automatises*, vol. 58, no. 1, p.75, 2025, https://doi.org/10.18280/jesa.580109.

[27] S. Huang, L. Xiong, J. Wang, P. Li, Z. Wang, and M. Ma, "Fixed-time synergetic controller for stabilization of hydraulic turbine regulating system," *Renewable energy*, vol. 157, pp.1233-1242, 2020, https://doi.org/10.1016/j.renene.2020.05.071.

[28] L. Zhang, Y. Wang, Y. Hou, and H. Li, "Fixed-time sliding mode control for uncertain robot manipulators," *IEEE Access*, vol. 7, pp.149750-149763, 2019, https://doi.org/10.1109/ACCESS.2019.2946866.

[29] A. Polyakov, "Nonlinear feedback design for fixed-time stabilization of linear control systems," *IEEE transactions on Automatic Control*, vol. 57, no. 8, pp.2106-2110, 2011, https://doi.org/10.1109/TAC.2011.2179869.

[30] S. Sengupta, S. Basak, and A. Peters, “Particle swarm optimization: A survey of historical and recent developments with hybridization perspectives,” *Machine Learning and Knowledge Extraction*, vol. 1, no. 1, pp. 157–191, 2018, https://doi.org/10.3390/make1010010.

[31] S. Jabber, S. Hashem, and S. Jafer, "Analytical and Comparative Study for Optimization Problems," *Iraqi Journal of Computers, Communications, Control and Systems Engineering*, vol. 23, no. 4, 46-57, 2023, https://doi.org/10.33103/uot.ijccce.23.4.5.

[32] K. Reddy and K. Saha, “A review of swarm-based metaheuristic optimization techniques and their application to doubly fed induction generator,” *Heliyon*, vol. 8, no. 10, p. e10956, 2022, https://doi.org/10.1016/j.heliyon.2022.e10956.

[33] S. Tahcfulloh, D. Maulianawati, and D. Wiharyanto, “Optimizing 2.4GHz Wireless Networks in Shrimp Ponds with Particle Swarm Optimization,” *Jurnal Ilmiah Teknik Elektro Komputer dan Informatika*, vol. 10, no. 4, pp. 817–832, 2024, https://doi.org/10.26555/jiteki.v10i4.30236.

[34] A. K. Ahmed, L. K. Majeed, S. Al-Wais, and H. Al-Khazraji, “Sliding mode position tracking control-based waterwheel plant algorithm for elbow rehabilitation systems," *International Journal of Robotics and Control Systems*, vol. 6, no. 2, pp.1164-1180, 2026, https://doi.org/10.31763/ijrcs.v6i2.2708.

[35] S. W. Shneen, J. M. D. Alkhasraji, and M. Q. Sulttan, “Internet-based Control of Thermo-optical Plant Improvement based on the PID-GWO System,” *Journal Fuzzy System Control*, vol. 2, no. 3, pp. 197–202, 2024, https://doi.org/10.59247/jfsc.v2i3.257.

[36] H. Al-Rammahi and A. Y. Asaad, “A particle swarm optimization-enhanced support vector regression model for accurate prediction of concrete compressive strength using slump test data,” *Control Systems and Optimization Letters*, vol. 3, no. 3, pp. 272–279, 2025, https://doi.org/10.59247/csol.v3i3.224.

[37] M. A. Al-Ali, O. F. Lutfy and H. Al-Khazraj, "Investigation of optimal controllers on dynamics performance of nonlinear active suspension systems with actuator saturation," *Journal of Robotics and Control (JRC)*, vol. 5, no. 4, pp.1041-1049, 2024, https://doi.org/10.18196/jrc.v5i4.22139.

[38] M. J. Mohamed, and L. T. Rasheed, "Design of nonlinear PID and FOPID controllers for electronic throttle valve plate’s position," *Journal of Electrical and Computer Engineering*, vol. 2024, no. 1, p.9984750, 2024, https://doi.org/10.1155/2024/9984750.

[39] P. Chotikunnan, W. Khotakham, A. Wongkamhang, A. Nirapai, P. Imura, K. Roongpraser, R. Chotikunnan, and N. Thongpance, N. "Genetic Algorithm-Optimized LQR for Enhanced Stability in Self-Balancing Wheelchair Systems," *Control Systems and Optimization Letters*, vol. 2, no. 3, 327-335, 2024, https://doi.org/10.59247/csol.v2i3.161.

[40] V. C. Bui, V. Q. Le, A. N. Ngo, and C. H. Canh, “Firefly Algorithm-Based PID Optimization for Active Suspension Systems in Electric Vehicles,” *Journal of Fuzzy Systems and Control*, vol. 3, no. 2, pp. 142–148, 2025, https://doi.org/10.59247/jfsc.v3i2.311.

[41] M. N. Ajaweed, A. H. Issa, and M. T. Muhssin, “Design and implementation of an OFOPID controller for Iraqi two areas power system using ant-colony optimization algorithm,” *Iraqi Journal of Computers, Communications, Control and Systems Engineering*, vol. 26, no. 1, pp. 83–100, 2026, https://doi.org/10.33103/2617-3352.1519.

[42] H. Al-Khazraji, C. Cole, W. and Guo, "Multi-objective particle swarm optimisation approach for production-inventory control systems," *Journal of Modelling in Management*, vol. 13, no. 4, pp.1037-1056, 2018, https://doi.org/10.1108/JM2-02-2018-0027.

[43] W.C. Wang, W.C. Tian, D.M. Xu, and H.F. Zang, "Arctic puffin optimization: A bio-inspired metaheuristic algorithm for solving engineering design optimization," *Advances in Engineering Software*, vol. 195, p.103694, 2024, https://doi.org/10.1016/j.advengsoft.2024.103694.

[44] G. Gauri, M. Kashish, G. Shruti, S.A. Iqbal, and J. More, "Load Frequency Control of Multi-Area Power System Using Arctic Puffin Optimization," In *2025 IEEE 1st International Conference on Smart and Sustainable Developments in Electrical Engineering (SSDEE)*, pp. 01-05, 2025, https://doi.org/10.1109/SSDEE64538.2025.10968053.

[45] R. Firmansyah, P. D. Widayaka, M. R. Fahrezy, P. P. S. Saputra, and D. Septian, "Voltage Control of DC Microgrid using Arctic Puffin Optimization Algorithm for Tuning of Sliding Mode Control Gain," In *2024 Seventh International Conference on Vocational Education and Electrical Engineering (ICVEE)*, pp. 279-282, 2024, https://doi.org/10.1109/ICVEE63912.2024.10823965.

[46] A. K. Abdelaal, A. M. Shaheen, A. A. El-Fergany, and M. H. Alqahtani, "Sliding mode control based dynamic voltage restorer for voltage sag compensation," *Results in Engineering*, vol. 24, p.102936, 2024, https://doi.org/10.1016/j.rineng.2024.102936.

[47] A. Alkamachi, "Robust Speed Control of Permanent Magnet DC Motors Using an Arctic Puffin Optimized PI Controller and Nonlinear Disturbance Observer," *Buletin Ilmiah Sarjana Teknik Elektro*, vol. 8, no. 3, pp.684-698, 2026, https://doi.org/10.12928/biste.v8i3.15723.

[48] M. A. E. Mohamed, K. Jagatheesan, and B. Anand, “Modern PID/FOPID controllers for frequency regulation of interconnected power system by considering different cost functions,” *Scientific Reports*, vol. 13, no. 1, p. 14084, 2023, https://doi.org/10.1038/s41598-023-41024-5.

[49] S. Singh, V. P. Singh, A. Mathur, T. K. Bashishtha, S. Padmanaban, and T. Varshney, “Airport microgrid control using integral-of-absolute-error having high renewable penetration,” *Scientific Reports*, vol. 15, no. 1, p. 23550, 2025, https://doi.org/10.1038/s41598-025-04820-9.

[50] L. Majeed, S. Al-Wais, M. Mustafaa, H. Al-Khazraji, and R. Kadhim, "Cheetah-Optimizer-Based Nonlinear Controller for Single-Link Flexible-Joint Manipulators: A Comparative Simulation Study," *International Journal of Robotics and Control Systems*, vol. 6, no. 3, 2107-2122, 2026, https://doi.org/10.31763/ijrcs.v6i3.2576.